



Convenient green production of CeO₂ nanoparticles by the auto combustion method

Omnia Abd El-Dayem¹, Mostafa Y. Nassar¹, Hossam S. Jahin², Wagdy El-DougDoug¹
Hesham H. El-Feky¹

¹ Chemistry Department, Faculty of Science, Benha University, Benha, Egypt.

² Central Laboratory for Environmental Quality Monitoring, National Water Research Center, ElKanater El-Khayria, 13621, Egypt.

Corresponding author: E-mail address: hesham.elfeky@fsc.bu.edu.eg

Abstract:

The production of cerium oxide (CeO₂) nanoparticles was investigated using an innovative and straightforward combustion method. In this approach, cerium oxide nanoparticles were generated from the precursor Ce(NO₃)₃·6H₂O through a combustion technique that utilized varying concentrations of jojoba oil as a fuel agent. The synthesized nanoparticles were characterized through X-ray diffraction (XRD) and Fourier-transform infrared spectroscopy (FTIR). The XRD analysis indicated that the cerium oxide nanoparticles had a cubic structure, with an average particle size of approximately 38.97 nm when using 3 mL of oil and 75.56 nm with 5 mL of oil, demonstrating good crystallinity. The FT-IR spectrum clearly showed a significant presence of cerium oxide nanoparticles. Overall, the results suggest that the combustion method is an effective and cost-efficient technique for producing high-quality cerium oxide nanoparticles.

Keywords: CeO₂, Jojoba, Nanoparticles, Combustion.

1. Introduction

A significant global challenge is water pollution caused by dyes, which are among the most harmful contaminants. The toxic waste introduced by dyes not only poses

serious health risks to humans but also disrupts the ecological balance ⁽¹⁾. Cerium oxide, recognized for its various valence states and crystalline structures, has been

investigated for a wide range of applications, including electrical and electronic devices, catalysis, adsorption, optical systems, electrochemical applications, batteries, functional materials, energy storage, magnetic data storage, and sensing technologies ⁽²⁻⁵⁾. Reducing particle size and increasing the active surface area are crucial for improving the characteristics of nanomaterials and meeting the increasing demands across many applications. Reducing particle size can improve conductivity, as well as the electrical, sensing, and catalytic characteristics of nanomaterials ^(6, 7). A ceramic material with a cubic fluorite structure, cerium (CeO_2) is stable at ambient temperature and up to its melting point of 2700°C without undergoing any known crystallographic changes ⁽⁸⁾. Since aggregated particles might result in uneven mixing and reduced sinterability, many applications call for non-agglomerated nanoparticles. Due to the distinct physical and chemical characteristics of nano-sized particles compared to bulk materials, there has been a lot of attention lately in increasing catalytic activity, sinterability, and other qualities by reducing grain size to the nanometer scale ⁽⁹⁾. An important attribute of CeO_2 is its efficient redox sites ($\text{Ce}^{4+}/\text{Ce}^{3+}$) and its ability to facilitate

oxygen exchange⁽¹⁰⁾. Cerium oxide nanoparticles are synthesized using a variety of methods ⁽¹¹⁾. Hydrothermal synthesis, mechanochemical procedures, sonochemical techniques, combustion synthesis, sol-gel methods, semi-batch reactors, microemulsion techniques, and spray pyrolysis are among the few described synthesis methods for CeO_2 nanoparticles ⁽¹²⁾. Among the various chemical processes, the combustion method is notable for its simplicity, cost-effectiveness, and time efficiency compared to other techniques. This study aims to synthesize CeO_2 nanoparticles using the combustion route, focusing on producing cerium oxide with reduced dimensions and examining its morphological properties. This method presents several advantages, including affordability, ease of preparation, and potential for industrial applications. In this research, CeO_2 nanoparticles are synthesized from the precursor $\text{Ce}(\text{NO}_3)_3 \cdot 6\text{H}_2\text{O}$ using a combustion technique with jojoba oil as a fuel agent. The synthesis procedures and their parameters, including the medium's pH, temperature, cerium oxide source, templating agents, and their concentrations, have a major impact on the physicochemical characteristics of cerium oxide ⁽¹³⁾. X-ray diffraction (XRD) and Fourier-transform infrared spectroscopy

(FT-IR) were used to assess the optical and structural characteristics of the produced CeO_2 .

2. Material and Methods:

2.1. Materials :

A key ingredient in the creation of cerium oxide nanoparticles in this study was cerium nitrate hexahydrate ($\text{Ce}(\text{NO}_3)_3 \cdot 6\text{H}_2\text{O}$) jojoba oil. Because of its good solubility and stability, cerium nitrate hexahydrate ($\text{Ce}(\text{NO}_3)_3 \cdot 6\text{H}_2\text{O}$) is a frequently used precursor for creating cerium oxide nanoparticles. This chemical has a molecular weight of 434.22 g/mol and crystallizes as colorless to pale yellow. With a solubility of roughly 1754 g/L at 25°C, it is highly soluble in water and appropriate for a variety of chemical operations. To improve the stability and dispersibility of the final nanoparticles, jojoba oil—a naturally occurring plant-derived oil high in unsaturated fatty acids—was added during the manufacturing process. We purchased jojoba oil, acid red dye, and $\text{Ce}(\text{NO}_3)_3 \cdot 6\text{H}_2\text{O}$ from Alpha Chemika (Maharashtra, india).

2.2. Preparation of CeO_2 Nanoparticles

All analytically pure reagents were used exactly as supplied, requiring no additional purification. In this study, CeO_2 powder

was successfully synthesized using the combustion method, with $\text{Ce}(\text{NO}_3)_3 \cdot 6\text{H}_2\text{O}$ as the precursor and jojoba oil serving as the fuel agent. In order to increase the stability and dispersibility of the final nanoparticles, jojoba oil—a naturally occurring plant-derived oil that is high in unsaturated fatty acids—was added to the manufacturing process. The use of jojoba oil not only aids in preventing agglomeration but also contributes to the development of a shield surrounding the nanoparticles, which can improve their functional properties. CeO_2 nanoparticles were synthesized using a novel method as follows. A 0.01 M solution of Ce(III) nitrate was prepared by dissolving 4.3 g of $\text{Ce}(\text{NO}_3)_3 \cdot 6\text{H}_2\text{O}$ in 20 mL of distilled water in separate beakers. After that, a yellow precursor formed when jojoba oil was added dropwise in different quantities (3 mL and 5 mL) to the thoroughly agitated solution. To create nanocrystalline CeO_2 powder, the resultant CeO_2 was calcined for two hours at 600°C after being evaporated on a hot plate at around 70 to 80°C. A fine, dark yellow powder was obtained and carefully collected for further characterization.

3. Results and discussion

3.1. An analysis of the synthesized CeO₂ nano-adsorbent

3.1.1. XRD Studies

The crystalline phases and crystallite sizes were estimated using X-ray diffraction (XRD). The XRD patterns of CeO₂ nanoparticles made using (a) 3 mL of jojoba oil and (b) 5 mL of jojoba oil are shown in Figure 1. The powder XRD analysis of the fabricated CeO₂ nanoparticles using 3 mL of oil was conducted with monochromatic CuK α 1 radiation (wavelength 1.5406 Å) over an angular range of 2 θ from 10 to 80 degrees. The XRD profile revealed a series of diffraction peaks at 28.618°, 33.150°, 47.551°, 56.422°, 59.139°, 69.513°, 76.802°, 79.168° (fig. 1 (a)). CeO₂ NPs by (5 mL of oil) exhibit crystalline peaks at

2 θ values of 28.636°, 33.113°, 47.562°, 56.439°, 59.162°, 69.503°, 76.747°, 79.182° (fig. 1 (b)) Using standard data, the cubic fluorite structure of CeO₂ was determined.^(14, 15) The sharp XRD peaks suggested that the synthesized CeO₂ nanoparticles possess good crystalline quality. The following equation describes how the full width at half maximum (FWHM) and the Debye-Scherrer formula were used to estimate the average size of the ordered CeO₂ nanoparticles:

$$D = 0.9\lambda / \beta \cos \theta \quad (\text{Eq.1})$$

where θ is the Bragg angle, β is the line broadening at half maximum intensity

(FWHM) in radians, λ is the X-ray wavelength, and 0.9 is the shape factor. It was discovered that the annealed CeO₂ nanoparticles had an average size of between 38.97 and 75.56 nm.

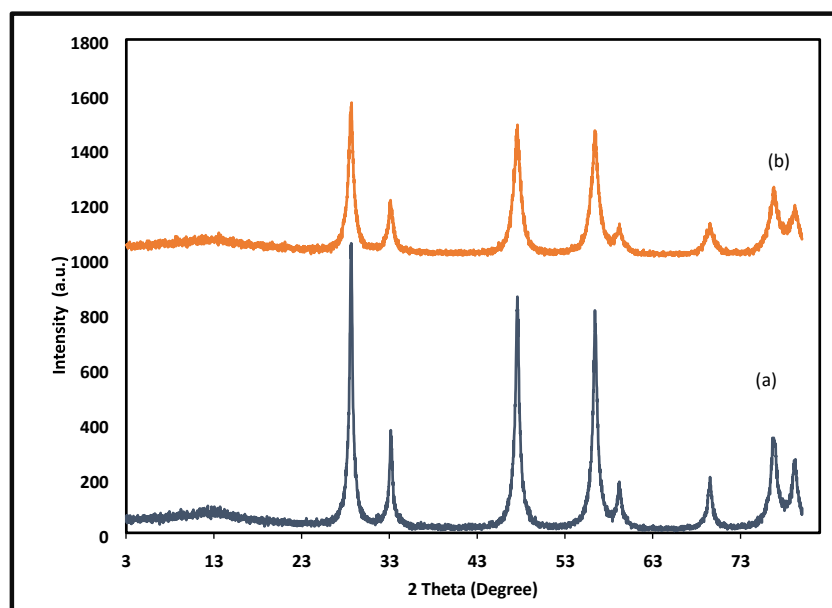


Fig.1. XRD plots of (a) CeO₂ NPs by (3ml of oil) , (b) CeO₂ NPs by (5ml of oil).

3.1.2. FT-IR Spectra Analysis

As illustrated in Figure 2, the produced CeO₂ nanoparticles' infrared spectrum (FTIR) covers the 400–4000 cm⁻¹ wavenumber range, aiding in the identification of the compound's functional groups and chemical bonds. The O-H stretching vibration in hydroxyl (OH⁻)

groups is responsible for the broad band at 3421.61 (a) and 3421.14 (b) cm⁻¹. Ce-O stretching vibration is represented by the strong band seen between 500 and 879 cm⁻¹ (16). Additionally, the peak at 1507.85 (a) and 1507.64 (b) cm⁻¹ is associated with the bending mode of water (H₂O).

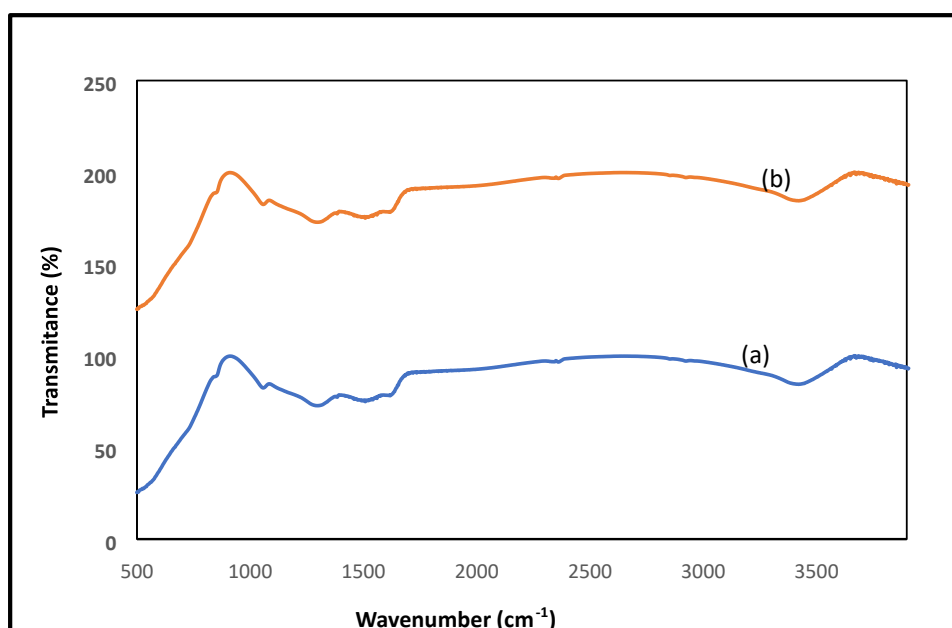


Fig.2. FT-IR spectra of the prepared Cerium oxide nanoparticles (a) by (3ml of oil) , (b) by (5ml of oil).

3.1.3. Adsorption Studies

Cerium oxide nanoparticles (CeO₂ NPs) have emerged as effective agents for eliminating dyes from contaminated water, particularly due to their photocatalytic properties. This study looks at how several factors affect CeO₂ NPs' effectiveness in dye adsorption and degradation processes.

n Important variables, such as pH, starting concentration, and adsorbent dose, were

systematically altered to evaluate their impact on the dye removal rate for substances such as Acid Red. The results indicated that lower pH levels significantly enhanced the adsorption capacity of the nanoparticles, promoting better interaction among the dye molecules and the CeO₂ surface. Additionally, increasing the dosage of cerium oxide nanoparticles improved degradation rates due to a higher

availability of active sites. These findings highlight the versatility of cerium oxide nanoparticles in water treatment applications and underscore the importance of optimizing operational conditions to maximize their effectiveness in dye removal. The following formulas were used to determine the cerium oxide adsorbent's removal effectiveness (R%):

$$(R \%) = (C_o - C_e) / C_o \times 100 \quad (\text{Eq.2})$$

where C_o (mg/L) is the Acid Red dye's starting concentration and C_e (mg/L) is the concentration at which the removal rate drops down significantly.

3.1.4. Effect of pH

One of the most important and influencing factors in dye adsorption is thought to be the pH of the solution. Thus, using an adsorbent dosage of 0.05 g and an initial dye

concentration of 50 mg/L, the adsorption of Acid Red dye onto the surface of the produced cerium oxide was investigated within a pH range of 3.52 to 10.01, adjusted using HCl and NaOH (0.1 M). Eq. 2 was used to determine the removal %, which was then displayed in Fig. 3 against the solution's initial pH variation.

The removal percentage increases as the initial pH rises from 3.52 to 5.08, reaching near saturation at pH 6.65, and then approaches approximately 86% at pH 9.54. This suggests enhanced efficiency of the nanocomposite formed between Acid Red dye and CeO_2 nanoparticles. The removal percentage consistently increases with rising initial pH. It is noteworthy that research investigating the impact of initial concentration and nanocomposite dose on Acid Red dye adsorption was carried out at an initial pH of 6.65.

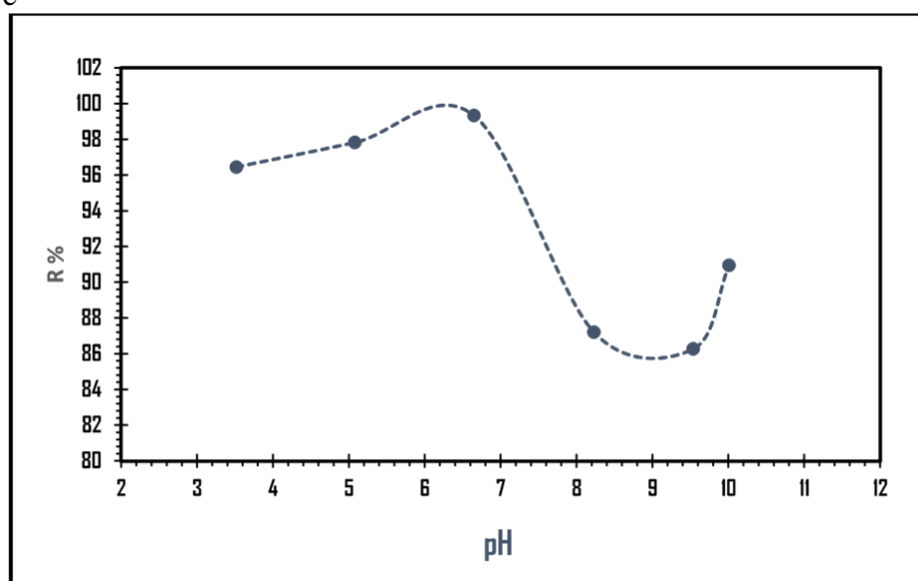


Fig. 3. Effect of pH on the efficiency of removing acid red dye using the as-prepared CeO_2 .

3.1.5. Adsorbent Dose

The impact of cerium oxide nanoparticles dosage on the removal percentage of Acid Red dye was investigated using a 50 mg/L Acid Red dye solution at pH 6.65. Figure 4 in the supporting information shows the absorbance spectra of Acid Red after treatment with various doses of nanoparticles. The nanoparticle dosage was varied from 0.00125 g/50 mL to 0.005 g/50 mL.

As the nanoparticle dosage grew from 0.00125 g to 0.005 g per 50 mL, the elimination percentage—which was determined from the obtained absorbance data using Eq. 2—rose from 38% to 99%. The increased availability of active adsorption sites on the surface of the nanoparticles at higher dosages is responsible for this notable increase in removal % with increasing nanoparticle dosage.

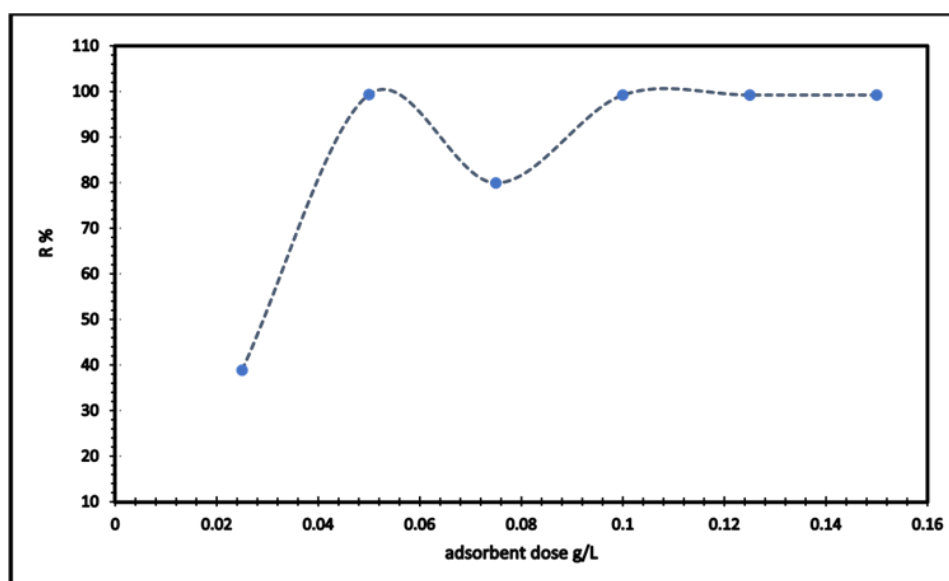


Fig. 4. Effect of adsorbent dose on the efficiency of removing acid red dye.

4. CONCLUSION

Nanocrystalline CeO_2 was successfully synthesized using the combustion method. A variety of analytical techniques were utilized to examine its structural, physical, and chemical properties. Jojoba oil was

used as a fuel agent in the combustion process to create CeO_2 nanoparticles from the precursor $\text{Ce}(\text{NO}_3)_3 \cdot 6\text{H}_2\text{O}$. With an average grain size of 38.97 nm for the sample containing 3 mL of oil and 75.56

nm for the sample containing 5 mL of oil, both annealed at 600°C, X-ray diffraction investigation verified the cubic (fcc) structure of CeO₂. According to Ce-O stretching vibration, Ce-O stretching modes were detected in CeO₂ between 500 and 879 cm⁻¹, according to FTIR measurements.

Acknowledgment

We wish to extend our sincere gratitude to the Egyptian Academy of Scientific Research and Technology, as well as the Faculty of Science at Benha University, for their generous funding and support of this research project. Their dedication to promoting scientific research and education has been vital in facilitating our work.

References

1. **S. Rajendran, T.A.K. Priya, K.S. Khoo, T.K.A. Hoang, H.-S. Ng, H.S.H. Munawaroh, C. Karaman, Y. Orooji, P.L. Show, A critical review on various remediation approaches for heavy metal contaminants removal from contaminated soils. *Chemosphere* 287, 132369 (2022) : A critical review on various remediation approaches for heavy metal contaminants removal from contaminated soils.** <https://doi.org/10.1016/j.chemosphere.2021.132369>
2. **M. Faisal, S.B. Khan, M.M. Rahman, and A. Jamal, *J. Mater. Sci. Technol.* 27 (2011) 594 : A Role of ZnO-CeO₂ Nanostructures as a Photo-catalyst and Chemi-sensor.** [https://doi.org/10.1016/S10050302\(11\)60113-8](https://doi.org/10.1016/S10050302(11)60113-8)
3. **S.B. Khan , M. Faisal , M.M. Rahman , and A. Jamal, *Sci. Tot. Environ.* 409 (2011) 2987: Exploration of CeO₂ nanoparticles as a chemi-sensor and photo-catalyst for environmental applications.** <https://doi.org/10.1016/j.scitotenv.2011.04.019>
4. **F. Niu et al., *Mater. Lett.* 63 (2009) 2132: Facile synthesis, characterization and low-temperature catalytic performance of Au/CeO₂ nanorods.** <https://doi.org/10.1016/j.matlet.2009.07.021>
5. **M. Palard, J. Balencie, A. Maguer, and J.F. Hochepped, *Mater. Chem. Phys.* 120 (2010) 79: Effect of hydrothermal ripening on the photoluminescence properties of pure and doped cerium oxide nanoparticles.** <https://doi.org/10.1016/j.matchemphys.2009.10.025>
6. **F. Meshkani and M. Rezaei, *Powder Tech.* 199 (2010) 144.O: Effect of process parameters on the synthesis of nanocrystalline magnesium oxide with**

- high surface area and plate-like shape by surfactant assisted precipitation method.
<https://doi.org/10.1016/j.powtec.2009.12.014>
7. **m O. Tunusoglu, R.M. Espi, U. Akbey, and M.M. Demir, Colloids Surf. A: Physicochem. Engin. Aspects 395 (2012):** Synthesis different sizes of cerium oxide CeO₂ nanoparticles by using different concentrations of precursor via sol-gel method.
<https://doi.org/10.1016/j.matpr.2021.09.452>
 8. **J.P. Holgado, R. Alvarez, and G. Munuera, Appl. Surf. Sci. 161 (2000) 301:** Study of CeO₂ XPS spectra by factor analysis: reduction of CeO₂.
[https://doi.org/10.1016/S0169-4332\(99\)00577-2](https://doi.org/10.1016/S0169-4332(99)00577-2)
 9. **G.D. Angel, J.M. Padilla, I. Cuauhtemoc, and J. Navarrete, J. Mol. Catal. A 281 (2008) 173:** Toluene combustion on γ -Al₂O₃-CeO₂ catalysts prepared from boehmite and cerium nitrate.
<https://doi.org/10.1016/j.molcata.2007.08.017>
 10. **S.A. Hassanzadeh-Tabrizi, E. Taheri-Nassaj, and H. Sar-poolaky, J. Alloys Comps. 456 (2008) 282:** Synthesis of an alumina-YAG nanopowder via sol-gel method.
<https://doi.org/10.1016/j.jallcom.2007.02.044>
 11. **Ketzial JJ, Nesaraj AS. Synthesis of CeO₂ nanoparticles by chemical precipitation and the effect of a surfactant on the distribution of particle sizes. Journal of Ceramic Processing Research. 2011;12(1):74–79:** Synthesis of CeO₂ nanoparticles by chemical precipitation and the effect of a surfactant on the distribution of particle sizes.
<http://dx.doi.org/10.36410/jcpr.2011.12.1.74>
 12. **W. Chen, F. Li, and J. Yu, Mater. Lett. 60 (2006) 57:** Combustion synthesis and characterization of nanocrystalline CeO₂-based powders via ethylene glycol-nitrate process.
<https://doi.org/10.1016/j.matlet.2005.07.088>
 13. **L. Giraldo, B. López, L. Pérez, S. Urrego, L. Sierra, M. Mesa, Mesoporous silica applications. Macromol. Symp. 258, 129–141 (2007) :** Mesoporous Silica Applications
<https://doi.org/10.1002/masy.200751215>
 14. **H. Yang, C. Huang, A. Tang, X. Zhang, and W. Yang, Mater. Res. Bulletin. 40 (2005) 1690 :** Microwave-assisted synthesis of ceria

nanoparticles..<https://doi.org/10.1016/j.materresbull.2005.05.014>

15. **K.L. Yu, G.L. Ruan, Y.H. Ben, and J.J. Zou, Mater. Sci. Engin. B. 139 (2007)197:** Convenient synthesis of CeO₂ nanotubes.
<https://doi.org/10.1016/j.mseb.2007.02.011>
16. **Z. Zhang, C. Kleinstreuer, J.F. Donohue, and C.S. Kim, J.Aerosol Sci. 36 (2005) 211:** Comparison of micro- and nano-size particle depositions in a human upper airway model.
<https://doi.org/10.1016/j.jaerosci.2004.08.006>